A Robust Approach for Active Distribution Network Restoration Based on Scenario Techniques Considering Load and DG Uncertainties

Xin Chen, Wenchuan Wu, *Senior Member, IEEE*, Boming Zhang, *Fellow, IEEE*, Xincong Shi

***Abstract*—Fluctuating outputs of distributed generations, time-varying load demands and estimation errors of loads bring substantial uncertainty risks to the active distribution network restoration, which becomes a challenge to the traditional deterministic algorithms. In this paper, a robust restoration approach is proposed to solve this issue, considering both DG outputs and load demands uncertainties. Firstly, a large number of simulation scenarios are generated according to the profiles of historical data. Then we employ the backward scenario reduction technique to cluster these scenarios for computational efficiency. Based on the set of reduced scenarios, the robust restoration control model is built to obtain robust expectedly optimal strategies, which is in the formulation of a mixed integer linear programming. Numerical tests implemented on a modified PG&E 69-bus system demonstrate the robustness and optimality of this proposed approach.**

***Index Terms*—active distribution network, uncertainty, robust restoration, scenario technique.**

I. Introduction

Automatic service restoration is one of the most important functions in the operation of distribution networks (DNs). Once a blackout event takes place, the outage power in unfaulted but out-of-service areas can be restored through tuning the status of branch switches, namely network reconfiguration. Till now, considerable studies have been devoted to develop fast and optimal restoration algorithms, including heuristic methods [1], expert systems [2], neutral network [3], mathematical programming [4], etc.

In the past decade, the rapid development of distributed generations (DGs) has been witnessed around the world, owing to the exhaustion of fossil fuels and global warming. With a large scale integration of wind power and photovoltaics to DNs, active distribution networks (ADNs) are formed to fully utilize the renewable resources and enhance the system reliability. In reality, it takes plenty of time to complete a restoration task due to the low level of automation. During this period, the DG outputs fluctuate along with the weather conditions, in addition to the constantly varying load demands in the connected areas. Besides, the estimations of loads mainly depend on the pseudo-measurement methods [5], whose errors are relatively large, because few real-time measurement devices are installed in present DNs. In summary, fluctuating DG outputs, time-varying load demands and estimation errors of loads are the three major uncertainty factors in ADN, introducing significant uncertainty risks and technical challenges to the ADN restoration.

However, the uncertainties of load demands and DG outputs have not been considered in most existing literatures, which are formulated as deterministic parameters in the restoration decision-making process. For ignoring the fluctuation of DG outputs and load demands, it may lead to poor restoration performance with a deterministic method under such uncertain conditions, even resulting in branches overloading or voltage violations. As a consequence, an originally feasible restoration scheme may turn infeasible, and it adversely affects the interruption duration and the number of outage customers, which are the uncertainty risks mentioned above. Although some papers [6] [7] apply fuzzy approaches to model the uncertainties, it is not in the sense of robustness, and how to determine appropriate membership functions is an intractable problem in reality. Our previous work [8] introduces a robust restoration decision-making model based on information gap decision theory, while it can only provide a specific Pareto optimal front associating with restoration strategies when confronting a certain fault, and the complete knowledge base of all these fronts is required in service.

In this paper, we propose a data-driven robust optimization ADN restoration approach based on scenario techniques, considering both DG uncertainties and load uncertainties, where the restoration decision-making problem is formulated as a mixed integer linear programming (MILP). The profiles of historical data are employed to construct the uncertainty sets of DG outputs and load demands, then we generate masses of simulation scenarios from them. In order to promote the computation efficiency, the backward scenario reduction technique [9] is utilized to cluster a large number of similar scenarios. In this manner, a set of reduced scenarios is obtained to represent the uncertain DG outputs and load demands in the restoration process. Furthermore, two extreme scenarios are supplemented to the set of reduced scenario for the sake of robust solutions. Numerical tests carried out on a modified PG&E 69-bus distribution system verify the robustness and optimality of our proposed method.

The remainder of this paper is organized as follows. In Section II, a deterministic restoration control (DRC) model is presented. In Section III, based on the scenario generation and

This work was supported by the National Key Basic Research Program of China (2013CB228206) and in part by the National Science Foundation of China (51477083)

X. Chen, W. Wu, B. Zhang are all with the Department of Electrical Engineering, State Key Laboratory of Power Systems, Tsinghua University, Beijing 100084, China (E-mail: wuwench@tsinghua.edu.cn). X. Shi is with Shanxi Electric Power Company, Taiyuan, China.

reduction techniques, we build the robust restoration control (RRC) model. Numerical tests are discussed in Section IV, and we draw conclusions in Section V.

II. Deterministic Restoration Control Model (DRC)

Essentially, the ADN restoration decision-making is an optimal switch combination problem with a number of operating constraints. Based on the studies in [8] [10], we build a deterministic restoration control (DRC) model with the mathematical programming method, for the reason that it can achieve the globally optimal solutions. Since the DG outputs and load demands are formulated as constant parameters in DRC model, it is a deterministic optimization model for ADN restoration indeed, which is presented as follows:

1) Objective Function:

$$Obj.\ \ \text{Max} \sum_{i \in \Psi_{out}} \tilde{P}_{L,i} \tag{1}$$

We aim to maximize the restored active power in objective function (1), where $\tilde{P}_{L,i}$ is the actual active load demand at bus *i* during the restoration period, and Ψ_{out} is the set of buses in the outage areas.

2) Radial Operation Constraint:

$$s.t. \begin{cases} y_{ij} \in \{0,1\}, \forall ij \in \Phi \\ \sum_{ij \in \Phi} y_{ij} = N_b - N_s \end{cases} \tag{2}$$

The binary variable y_{ij} is the decision variable and denotes the status of branch *ij*, which equals to 1 if branch *ij* is connected and equals to 0 otherwise. Φ is the set of all branches. N_b and N_s are the number of all buses and the number of substation buses respectively, while the corresponding equality ensures radial network topologies of the solutions.

3) Voltage Reference and Security Constraints:

$$\begin{cases} V_s = V_{ref} \\ U_i = V_i^2, \forall i \in \Psi \\ \underline{U}_i \le U_i \le \bar{U}_i \end{cases} \tag{3}$$

The voltage magnitude V_s at the substation bus is set as the reference. Ψ denotes the set of all buses. In order to linearize the quadratic voltage formulations, we let the squared voltage magnitude U_i at bus *i* to be the voltage variable instead of V_i. $\underline{U}_i$ and $\bar{U}_i$ are the lower and upper bounds of the squared voltage magnitude at bus *i*, respectively.

4) Branch Capacity Constraints:

$$P_{ij}^2 + Q_{ij}^2 \le y_{ij} \cdot \bar{S}_{ij}^2, \forall ij \in \Phi \tag{4}$$

P_{ij} and Q_{ij} are the active and reactive power flow of branch *ij* from bus *i* towards bus *j*, respectively. $\bar{S}_{ij}^2$ is the apparent power capacity of branch *ij*, which multiplies y_{ij} to limit the power flow to zero in disconnected branches. Actually, equation (4) is a quadratic circular constraint, and it can be linearized in the linearization approach shown as Fig. 1, where several square constraints are utilized to approximate the circular constraint. As for engineering applications, two square constraints (5) with a rotation angle at 45 degrees are accurate enough to substitute for (4). Generally, we can use more square constraints to improve the level of precision in this approximation.

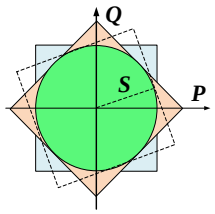

Fig. 1 The circular constraint linearization method.

$$\begin{cases} -y_{ij} \cdot \bar{S}_{ij} \le P_{ij} \le y_{ij} \cdot \bar{S}_{ij}, \forall ij \in \Phi \\ -y_{ij} \cdot \bar{S}_{ij} \le Q_{ij} \le y_{ij} \cdot \bar{S}_{ij} \\ -\sqrt{2} y_{ij} \cdot \bar{S}_{ij} \le P_{ij} + Q_{ij} \le \sqrt{2} y_{ij} \cdot \bar{S}_{ij} \\ -\sqrt{2} y_{ij} \cdot \bar{S}_{ij} \le P_{ij} - Q_{ij} \le \sqrt{2} y_{ij} \cdot \bar{S}_{ij} \end{cases} \tag{5}$$

5) Power Flow Equality Constraints:

For the branch power flow equality constraints, we have

$$\begin{cases} U_i - U_j \le 2\left(P_{ij} R_{ij} + Q_{ij} X_{ij}\right) + M \cdot \left(1 - y_{ij}\right) \\ U_i - U_j \ge 2\left(P_{ij} R_{ij} + Q_{ij} X_{ij}\right) - M \cdot \left(1 - y_{ij}\right) \\ \forall ij \in \Phi \end{cases} \tag{6}$$

We derive (6) from the *Distflow* model [11], ignoring the power loss in networks. R_{ij} and X_{ij} are the resistance and reactance of branch *ij*, respectively. *M* denotes a very big positive number, which is utilized to remove the power flow constraints in disconnected branches.

For the bus power equality constraints, we have

$$\begin{cases} \sum_{j \in i} P_{ji} = P_{L,i}, \sum_{j \in i} Q_{ji} = Q_{L,i} \\ P_{L,i}, Q_{L,i} \ge \varepsilon, \forall i \in \Psi_{con} \end{cases} \tag{7}$$

$$\begin{cases} \sum_{j \in i} P_{ji} = \tilde{P}_{L,i}, \sum_{j \in i} Q_{ji} = Q_{L,i}^E / P_{L,i}^E \cdot \tilde{P}_{L,i} \\ P_{L,i}^E \ge \tilde{P}_{L,i} \ge \varepsilon, \forall i \in \Psi_{out} \end{cases} \tag{8}$$

$$\begin{cases} \sum_{j \in i} P_{ij} = \tilde{P}_{G,i}, \sum_{j \in i} Q_{ij} = Q_{dg,i}^E / P_{dg,i}^E \cdot \tilde{P}_{G,i} \\ P_{G,i}^m \ge \tilde{P}_{G,i} \ge \varepsilon, \ \forall i \in \Psi_{DG} \end{cases} \tag{9}$$

where $j \in i$ denotes all the buses *j* which are connected to bus *i*. Ψ_{con}, Ψ_{out} and Ψ_{DG} are the set of buses in the connected areas, the set of buses in the outage areas and the set of DG buses, respectively. $P_{L,i}$ and $Q_{L,i}$ are the active and reactive load demand at bus *i*, respectively, while the same notations with a tilde, like $\tilde{P}_{L,i}$, mean that they are not parameters but variables. $\tilde{P}_{G,i}$ and $P_{G,i}^m$ are the actual active output and the maximum active output of DG bus *i*, respectively. The notations with a superscript of *E* denote the expected values during the restoration period, such as $P_{L,i}^E$. Here, ε represents a very small positive number, and the corresponding inequalities aim at avoiding the existence of transfer buses with no power injection. In (8) and (9), the constant power factors of load de-

mands and DG outputs are assumed.

From the formulation of DRC model, a mixed integer linear programming (MILP) is observed. Because the performances of modern MILP solvers based on the integration between branch-and-bound and cutting-plane algorithms have been significantly improved, it is a competitive approach in computational efficiency against other restoration algorithms.

III. Robust Restoration Optimization Algorithm

Based on DRC model, we take the uncertainties of DG outputs and load demands into consideration, and build the robust restoration control (RRC) model using scenario techniques in this section.

A. Scenarios generation and reduction method

According to the profiles of historical data, the uncertainty sets of DG outputs and load demands are established as Ω:

$$\Omega=\begin{cases}\tilde{P}_{L,i} \in \left[\underline{P}_{L,i},\bar{P}_{L,i}\right], \forall i \in \Psi_{con} \\ \tilde{P}^{m}_{G,i} \in \left[\underline{P}^{m}_{G,i},\bar{P}^{m}_{G,i}\right], \forall i \in \Psi_{DG}\end{cases} \tag{10}$$

Meantime, the corresponding empirical covariance $\left\{\sigma^{2}_{L,i},\sigma^{m,2}_{G,i}\right\}$ can be calculated with the given samples of historical data. Here, we suppose that the actual DG outputs and load demands follow normal distributions, which are shown as expression (11):

$$\begin{cases}\tilde{P}_{L,i} \sim \boldsymbol{N}\left(P^{E}_{L,i},\sigma^{2}_{L,i}\right), \forall i \in \Psi_{con} \\ \tilde{P}^{m}_{G,i} \sim \boldsymbol{N}\left(P^{E,m}_{G,i},\sigma^{m,2}_{G,i}\right), \forall i \in \Psi_{DG}\end{cases} \tag{11}$$

where $P^{E}_{L,i}$ and $P^{E,m}_{G,i}$ are the expected load demands and expected DG maximum outputs. After that, we can generate plenty of simulation scenarios randomly and independently based on the distribution functions (11), while the generated values should be within the uncertainty sets (10).

However, the computational effort for solving scenario-based optimization models heavily relies on the number of scenarios. To relieve the huge computation burden with a good approximation, we use the backward scenario reduction technique described in [12] to cluster scenarios, and the procedures of this method are presented as follows:

1) Initialization: Supposing that the number of generated scenarios is *N*, and the initial probability of each scenario s is set to 1/*N*. Denoting the original scenario set as φ and the target reduced scenario set as φ_*.

2) Computing Kantorovich Distance (KD): Compute the KD for each pair of scenarios and construct the KD matrix comprising all the scenarios and associated distance to each other. The KD between two scenarios s_i and s_j is defined as:

$$\mathrm{KD}_{ij}=\left\|s_i-s_j\right\|_2 \tag{a}$$

3) Marking Nearest Scenario: For each scenario s_i, locate the other nearest scenario, namely the scenario s_j ($j \neq i$) with the minimum KD_{ij} in the KD matrix.

4) Computing Probability KD (PKD): For each pair of scenarios marked in step *3)*, compute their PKD:

$$\mathrm{PKD}_{ij}=\min_{j}\left\{\mathrm{KD}_{ij}\right\}\times \mathrm{Pr}_i \tag{b}$$

where Pr_i is the probability of scenario s_i. Next, compare PKD_{ij} for all scenario pairs in the KDM, and the assessed scenario s_i which has the minimum value will be eliminated. Meanwhile, add the probability of the eliminated s_i to the probability of the nearest scenario s_j:

$$\mathrm{Pr}_j=\mathrm{Pr}_i+\mathrm{Pr}_j \tag{c}$$

Reconstruct the KD matrix after one scenario is removed.

5) Checking for Termination: Repeat steps *2)–4)* to eliminate one scenario in each iteration until the desired number of the target reduced scenario set is met.

In this scenario reduction approach, we can obtain a small scale scenario set φ_* with reasonably good approximation, which is used to simulate the uncertainties of DG outputs and load demands during the ADN restoration. The probability of each scenario in this set is known as well.

B. Robust Restoration Control Model (RRC)

To make the expression explicit, we redescribe the DRC model in a compact form as follows.

$$Obj.\ \max_{\boldsymbol{y}}\ \boldsymbol{c}^{\mathrm{T}}\boldsymbol{x} \tag{12}$$

$$s.t.\quad \boldsymbol{A}\boldsymbol{x} \le \boldsymbol{b} \tag{13}$$

$$\boldsymbol{B}\boldsymbol{x}+\boldsymbol{C}\boldsymbol{y} \le \boldsymbol{g} \tag{14}$$

where the vector $\boldsymbol{x}$ denotes the power flow variables $\left\{P_{ij},Q_{ij},U_i\right\}$, and the switching vector $\boldsymbol{y}$ represents the status of each branch $\left\{y_{ij}\right\}$. Equation (14) depicts the operating constraints associated with the switching vector $\boldsymbol{y}$, while the remaining constraints are expressed as (13). The matrices $\boldsymbol{A}$, $\boldsymbol{B}$, $\boldsymbol{C}$ and the vectors $\boldsymbol{c}$, $\boldsymbol{b}$, $\boldsymbol{g}$ are the parameters of distribution networks. It should be noted that the equality equations of power balance are reformulated in an equivalent unified form as inequalities for simplicity.

To ensure the robustness of solutions, two extreme scenarios are supplemented to the scenario set φ_*, which are the combinations of heaviest load demands/lightest DG outputs and heaviest DG outputs/lightest load demands within the uncertainty sets (10), forming an expanding scenario set as:

$$\varphi^{E}_{*}=\varphi_{*}\cup\left\{\left(\bar{P}_{L,i},\underline{P}^{m}_{G,i}\right),\left(\underline{P}_{L,i},\bar{P}^{m}_{G,i}\right)\right\} \tag{15}$$

Then, our robust restoration control model is established as follows:

$$Obj.\ \max_{\boldsymbol{y}}\ \sum_{s\in\varphi_*}\left(\mathrm{Pr}_s\cdot\boldsymbol{c}^{\mathrm{T}}\boldsymbol{x}_s\right) \tag{16}$$

$$s.t.\begin{cases}\boldsymbol{A}\boldsymbol{x}_s \le \boldsymbol{p}_s, \forall s \in \varphi^{E}_{*} \\ \boldsymbol{B}\boldsymbol{x}_s+\boldsymbol{C}\boldsymbol{y} \le \boldsymbol{g}_s\end{cases} \tag{17}$$

The objective function (16) aims to maximize the expected restored power under the reduced scenarios φ_*, where Pr_s denotes the probability of scenario s. Due to the constraints (17), the restoration strategy solutions $\boldsymbol{y}$ can keep feasible and robust for all the scenarios in the set φ^{E}_{*}.

The proposed RRC model is in the formulation of MILP as well, which can be solved efficiently via many commercially available optimizers.

IV. Numerical Tests

A. Test System and Parameters Setting.

A modified PG&E 69-bus distribution system, shown as Fig.2, is used for numerical tests. The dash red lines represent the link lines that are usually open, while the yellow diamonds denote the photovoltaics (PV) buses. The voltage magnitude of bus-1 is set to 10.5kV as the reference. Detailed parameters and configurations of this modified PG&E 69-bus system are available online [13].

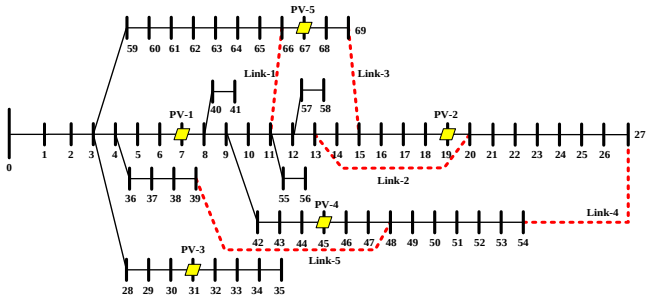

Fig. 2 The modified PG&E 69-bus distribution system.

Meantime, it is assumed that the uncertainty sets and the normal distributions of uncertain load demands and PV outputs are established as expression (18) and (19) respectively, according to the historical data. Then we generate 3000 simulation scenarios randomly and reduce them to 22 selected scenarios, comprising two extreme scenarios. Considering the correlation of the PVs located in neighboring areas, we use the same coefficient β to describe the uncertainties of all the PV outputs during the scenario generation process.

$$\Omega=\begin{cases}\tilde{P}_{L,i} \in \left[\ 0.8P^{E}_{L,i}\ ,\ 1.2\,P^{E}_{L,i}\ \right], \forall i \in \Psi_{con} \\ \tilde{P}^{m}_{G,i} \in \left[0.84P^{E,m}_{G,i}, 1.16P^{E,m}_{G,i}\right], \forall i \in \Psi_{DG}\end{cases} \tag{18}$$

$$\begin{cases}\tilde{P}_{L,i}=\alpha_i P^{E}_{L,i}\ ,\ \alpha_i \sim \boldsymbol{N}\left(1\ ,\ 0.1^2\right), \forall i \in \Psi_{con} \\ \tilde{P}^{m}_{G,i}=\beta_i P^{E,m}_{G,i}, \beta_i \sim \boldsymbol{N}\left(1, 0.08^2\right), \forall i \in \Psi_{DG}\end{cases} \tag{19}$$

Since DRC model is a deterministic mathematical programming method with no regard to the uncertainties, it can serve as a striking contrast against the proposed RRC model in the following tests. In order to differentiate the restoration performances between DRC and RRC, we suppose that all branches in the test system can be operated, which contributes to a more complicated distribution network.

B. Tests in the Extreme Scenarios (ES).

To verify the robustness of RRC strategies, we compared the restoration performances of DRC model and RRC model under these two extreme scenarios (ESs) mentioned above. Here, ES-1 denotes the conditions with the heaviest load demands (α_i=1.2) and the lightest PV outputs (β_i=0.84), while ES-2 is just the reverse (α_i=0.8 β_i=1.16).

In the case of faults occurring in branch ln10-11, it caused 0.7401MW outage loads in the downstream of this feeder. After faults isolation, the restoration strategies generated via DRC model and RRC model were conducted to restore loads, respectively. In ES-2, both DRC strategy and RRC strategy came to success and recovered all the outage power. However, DRC strategy became infeasible for violating the voltage constraints under ES-1. To fulfill DRC restoration scheme, additional 0.027MW loads shedding was deemed to happen at least. While RRC strategy survived ES-1 and still achieved the optimal restored power.

The detailed results are presented in TABLE I.

TABLE I
Restoration Results of RRC and DRC of ln10-11 under the Extreme Scenarios

Method	Restored Power (MW)		Disconnected Branches in Restoration Strategy
	ES-1	ES-2	
RRC	0.7401	0.7401	ln13-20, ln15-69, ln27-54, ln39-48.
DRC	-0.027	0.7401	ln11-12, ln13-14, ln53-54, ln39-48.

To further illustrate the restoration characteristics of the proposed RRC model, we undertook an "N-1" scan process on the test system under the extreme scenarios. Skipping the cases with no restorable loads, the comparisons in recovery power between DRC and RRC are shown as Fig.3.

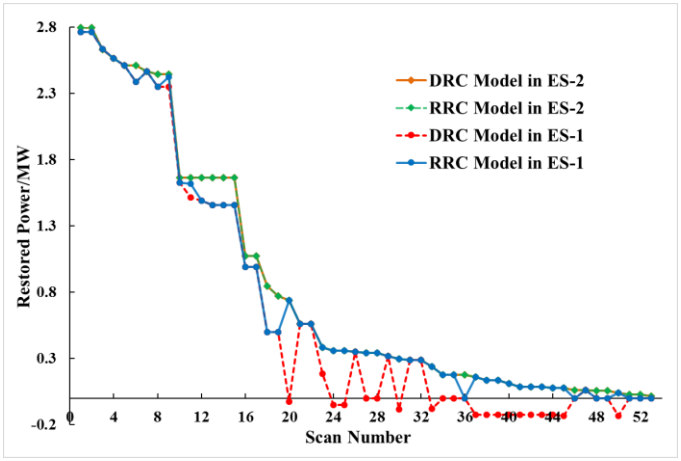

Fig. 3 The comparisons in restored power between DRC and RRC in "N-1" scan process under the extreme scenarios. The x-axis is the scan number in decreasing order of the restored power under ES-2. The y-axis is the final restored power, in units of MW.

From Fig.3, it is recognized that ES-2 has no evident effects on the restoration consequences, when DRC model and RRC model succeed with the same good performances, shown as the orange and green curves respectively. In terms of ES-1, DRC strategies failed many times and led to additional load shedding (negative restored power), depicted as the red curve in Fig.3. In contrast, RRC strategies kept feasible and optimal in all cases with better performances than DRCs' under ES-1, shown as the blue curve. Generally, branch overloading tends to violate the voltage and thermal constraints easily. Because the penetration ratio of PV is low in our test system, the restoration results mainly rely on the fluctuation of load demands. Hence, ES-1 with the heaviest loads represents the worst-case

scenario for restoration in some degree, challenging the deterministic method DRC, while RRC model is immune to the extreme scenarios for its robustness.

The aggregate results of this scan under ES-1 are summarized as TABLE II. It is observed that the infeasible ratio of RRC model was consistently zero, with a greater total restored power than DRC model.

TABLE II
RESTORATION RESULTS OF "N-1" SCAN UNDER ES-1

Method	Infeasible Times	Infeasible Ratio	Total Restored Power/MW
RRC	0	0	41.76
DRC	19	41.3%	35.81

C. Monte Carlo Simulation Tests.

Monte Carlo simulations were utilized to simulate the normal conditions for restoration, and another "N-1" scan process was carried out. In case of each fault, we generated 2000 sampling scenarios independently and randomly within the 3δ intervals of the uncertainty sets (18), when DRC strategies and RRC strategies were implemented to recover outage loads. From the results of this scan, it was seen that RRC strategies remained feasible in all cases, with no less expected restored power than DRCs' at all times. Several cases with distinct outcomes between DRC and RRC are presented in TABLE III, when RRC performed much better than DRC in the infeasible ratio and the expected recovery power for its robustness.

TABLE III
MONTE CARLO SIMULATION RESULTS OF DRC AND RRC

Faulty Branch	Method	Infeasible Times	Infeasible Ratio	Expected Restored Power/MW
ln19to20	RRC	0	0	0.1765
	DRC	5	0.25%	0.1747
ln60to61	RRC	0	0	0.1338
	DRC	24	1.2%	0.1314
ln63to64	RRC	0	0	0.0857
	DRC	26	1.3%	0.0842
ln68to69	RRC	0	0	0.0392
	DRC	22	1.1%	0.0385
ln38to39	RRC	0	0	0.3847
	DRC	0	0	0.3836

D. Computational Efficiency.

The MILP based robust network restoration model solved with IBM ILOG CPLEX software (ver.12.5). The test environment was a laptop with an Intel Core i7-4510U 2.60-GHz processor and 8 GB of RAM. The average CPU time for completing a model building and solution procedure in the modified PG&E 69-bus system is presented as TABLE IV.

TABLE IV
COMPUTING TIME FOR DRC MODEL AND RRC MODEL

Method	DRC	RRC with 12 reduced scenarios	RRC with 22 reduced scenarios	RRC with 52 reduced scenarios
CPU Time/s	2.3	20.1	48.8	259.6

The computing time of RRC model increases significantly with more scenarios, however a dozen of representative scenarios are sufficient for obtaining robust restoration strategies.

V. CONCLUSIONS

To address the uncertainty risks existing in the ADN restoration, we propose a robust restoration control (RRC) model based on the scenario techniques, formulated as a mixed integer linear programming. The simulations of this robust approach are carried out on a modified PG&E 69-bus distribution system, and the test results illustrate that RRC strategies can always keep feasible under the uncertain conditions. Through the comparisons against a deterministic restoration control (DRC) model, the robustness and optimality of our RRC model are verified.

VI. REFERENCES

[1] S. Toune, H. Fudo, T. Genji, Y. Fukuyama, Y. Nakanishi, "Comparative study of modern heuristic algorithms to service restoration in distribution systems," IEEE Trans. Power Del., vol. 17, no. 1, pp. 173-181, Jan 2002.

[2] C.S. Chen, C.H. Lin, T.T. Ku, M.S. Kang, C.Y. Ho, C.F. Chen, "Rule-based expert system for service restoration in distribution automation systems, "in 2012 IEEE International Conference on Power System Technology (POWERCON), pp. 1-6, Oct. 30 2012-Nov. 2 2012.

[3] Y. Huang, S. Chen, C. Huang, "Evolving radial basic function neural network for fast restoration of distribution systems," in 2011 6th IEEE Conference on Industrial Electronics and Applications (ICIEA), pp. 401-406, 21-23 June 2011.

[4] R.A. Jabr, R. Singh, B.C. Pal, "Minimum Loss Network Reconfiguration Using Mixed-Integer Convex Programming," IEEE Trans. Power Syst., vol. 27, no. 2, pp. 1106-1115, May 2012.

[5] R. Singh, B. C. Pal, R. A. Jabr. Distribution system state estimation through Gaussian mixture model of the load as pseudo-measurement[J]. IET generation, transmission & distribution, 2010, 4(1): 50-59.

[6] D. S. Popovic, Z. N. Popovic, "A risk management procedure for supply restoration in distribution networks," IEEE Trans. Power Syst., vol. 19, no. 1, pp. 221-228, Feb. 2004.

[7] H.-C. Kuo, Y.-Y. Hsu, "Distribution system load estimation and service restoration using a fuzzy set approach," IEEE Trans. Power Del. vol. 8, no. 4, pp. 1950-1957, Oct 1993.

[8] K. Chen, W. Wu, B. Zhang, H. Sun, "Robust Restoration Decision-Making Model for Distribution Networks Based on Information Gap Decision Theory," IEEE Trans. on Smart Grid, vol. 6, no. 2, pp. 587-597, Feb., 2015.

[9] Gröwe-Kuska N, Heitsch H, Römisch W. Scenario reduction and scenario tree construction for power management problems[C]//Power Tech Conference Proceedings, 2003 IEEE Bologna. IEEE, 2003, 3: 7 pp. Vol. 3.

[10] J.A. Taylor, F.S. Hover, "Convex Models of Distribution System Reconfiguration," IEEE Trans. Power Syst., vol. 27, no. 3, pp. 1407-1413, Aug. 2012.

[11] Baran M E, Wu F F. Optimal sizing of capacitors placed on a radial distribution system[J]. Power Delivery, IEEE Transactions on, 1989, 4(1): 735-743.

[12] Razali N M M, Hashim A H. Backward reduction application for minimizing wind power scenarios in stochastic programming[C]//Power Engineering and Optimization Conference (PEOCO), 2010 4th International. IEEE, 2010: 430-434.

[13] (Nov. 8, 2015). [Online]. Available: https://drive.google.com/file/d/0BzBNHekT7PzcUlpkVXpHc0JXcm8/view?usp=sharing.